

Visible-Light-Driven BiOI-Based Janus Micromotor in Pure Water

Renfeng Dong,[†] Yan Hu,[‡] Yefei Wu,[‡] Wei Gao,[§] Biye Ren,^{*,‡,†} Qinglong Wang,[†] and Yuepeng Cai^{*,†,†}

[†]School of Chemistry and Environment, Guangzhou Key Laboratory of Materials for Energy Conversion and Storage, Guangdong Provincial Engineering Technology Research Center for Materials for Energy Conversion and Storage, South China Normal University, Guangzhou 510006, China

[‡]School of Materials Science and Engineering, South China University of Technology, Guangzhou 510640, China

[§]Department of Electrical Engineering & Computer Sciences, and Berkeley Sensor and Actuator Center, University of California, Berkeley, California 94720, United States

S Supporting Information

ABSTRACT: Light-driven synthetic micro-/nanomotors have attracted considerable attention due to their potential applications and unique performances such as remote motion control and adjustable velocity. Utilizing harmless and renewable visible light to supply energy for micro-/nanomotors in water represents a great challenge. In view of the outstanding photocatalytic performance of bismuth oxyiodide (BiOI), visible-light-driven BiOI-based Janus micromotors have been developed, which can be activated by a broad spectrum of light, including blue and green light. Such BiOI-based Janus micromotors can be propelled by photocatalytic reactions in pure water under environmentally friendly visible light without the addition of any other chemical fuels. The remote control of photocatalytic propulsion by modulating the power of visible light is characterized by velocity and mean-square displacement analysis of optical video recordings. In addition, the self-electrophoresis mechanism has been confirmed for such visible-light-driven BiOI-based Janus micromotors by demonstrating the effects of various coated layers (e.g., Al₂O₃, Pt, and Au) on the velocity of motors. The successful demonstration of visible-light-driven Janus micromotors holds a great promise for future biomedical and environmental applications.

Nano- and microscale devices powered by biocompatible and environmentally friendly fuel sources are strongly desired for practical applications.¹ However, most systems reported so far, such as bimetallic catalytic nanowires,² microtubular microrockets,³ Janus microspheres,⁴ and supermolecule-based nanomotors,⁵ require toxic chemicals (H₂O₂, I₂, N₂H₄) as fuels which are not appropriate for *in vivo* use. As a result, autonomous nanomotors that can be self-propelled in biofluids has recently been developed.⁶ Meanwhile, considerable efforts have been devoted to motors that can be powered by external stimuli such as magnetic fields,⁷ electrical fields,⁸ ultrasound,⁹ and light.¹⁰ Light is one of the most efficient and versatile physical stimuli to facilitate and regulate the propulsion of micro-/nanomotors. Several light-driven micro-/nanomotors have been reported recently, such as TiO₂-based micromotors propelled by photocatalytic activities,¹¹ polymer-based microrockets driven by photothermal

effects,¹² and organic microswimmers activated by photoisomerizations.¹³ However, to the best of our knowledge, in pure water, all reported light-driven motors are propelled autonomously under either ultraviolet (UV) or near-infrared (NIR) light. UV light accounts for only 4% of the incoming solar energy and is shown to be harmful to human beings,¹⁴ while high-intensity NIR dramatically changes local temperature and could induce cell damage due to the thermal radiation, greatly limiting its wide application.¹⁵ Visible light accounts for about 43% of the incoming solar energy,¹⁶ and it is necessary in human daily life. Thus, it can potentially serve as an ideal external stimulus for propelling micromotors. In order to expand the applications of synthetic micromotors, overcoming the challenges of using visible light to supply energy for micromotors' self-propulsion in biocompatible environments has become critically important.

Bismuth oxyiodide (BiOI)—one of the most common photocatalysts which can be activated by visible light due to its narrow band gap (1.7 eV)¹⁷—is of immense importance owing to its excellent optical and electrical properties. It has been widely applied in numerous fields ranging from pollutant degradation¹⁸ and bacteria disinfection¹⁹ to solar cells.²⁰ Moreover, it is well established that metal junctions can greatly enhance the photocatalytic activity of semiconductors due to an efficient electron–hole separation.²¹

In light of these advantages, herein we present visible light powered Janus micromotors based on BiOI microspheres with one hemisphere coated with a metal layer, propelled by self-electrophoresis mechanism (Figure 1A). Upon exposure to visible light, electrons from the BiOI conduction band are trapped into the metal layer, resulting in a net negative charge at the metal side, while at the BiOI side, H⁺ ions are produced from the oxidation of water and highly concentrated on the surface.²² In order to balance the electrical charge, the H⁺ ions migrate within the double layer formed at the surface of the micromotor in pure water from the BiOI side toward the metal side. There, the H⁺ ions are consumed in the reduction half-reaction, completing the photochemical reaction. The net movement of H⁺ ions are accompanied by a corresponding electroosmotic flow of water molecules to the metal side, causing a net displacement of the particle and propels the BiOI

Received: September 20, 2016

Published: January 24, 2017

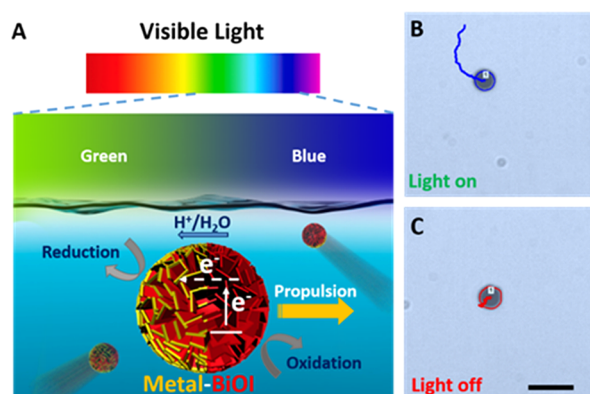
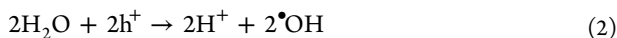


Figure 1. (A) Schematic of visible-light-driven BiOI-metal Janus micromotors. (B,C) Tracklines (taken from Video S1) illustrating the distance traveled by the micromotors under level 1 green light (43 900 lux) and level 5 green light (background light, 100 lux) over 30 s, respectively. Scale bar: 5 μm . Details about light levels are described in the Supporting Information.

micromotor with BiOI side forward. To date, most reports on BiOI photocatalysts are focused on the decomposition of liquid organic pollutants.²² According to literature,²² a possible catalytic cycle under visible light is given below:

For the BiOI side:



For the gold side:



Such electrophoresis mechanism is similar to that of classic bimetal catalytic nanomotors,^{2a} however, here, the self-electrophoresis is triggered by visible light. Since the propulsion of BiOI-based Janus micromotors is activated by visible light exposure, motors exhibit active directional motion under green light due to the self-electrophoretic effect (Figure 1B). In contrast, only extremely weak motion is observed in the absence of green light (Figure 1C). To the best of our knowledge, this is the first demonstration of visible-light-driven Janus micromotors that can be operated in a fully biocompatible environment using only visible light as external stimuli and pure water as fuel without addition of any other chemicals. Such visible-light-driven propulsion is very attractive, especially considering the toxicity of common used chemical fuels (e.g., H_2O_2) and the potential harm from UV or NIR light.

BiOI microspheres are fabricated according to previously reported methods²³ and characterized by the scanning electron microscopy (SEM) (Figure S1A), X-ray diffraction (XRD) (Figure S1B), and X-ray photoelectron spectroscopy (XPS) (Figure S1C) in detail. The results indicate that these BiOI microspheres are reliable for fabricating visible-light-driven BiOI-based Janus micromotors. The BiOI-based Janus micromotors are prepared by coating a thin metal film (thickness: 40 nm) on a hemisphere of the BiOI particles. It is clear from Figure 2A that the edges of uncoated BiOI flakes are sharper than Au-coated flakes. The energy-dispersive X-ray (EDX) results further confirm the Janus structure of such motors (Figure 2B,C).

In view of the visible-light-induced motion of BiOI-based Janus micromotors in pure water (Figure, 1A), cyclic “On” and

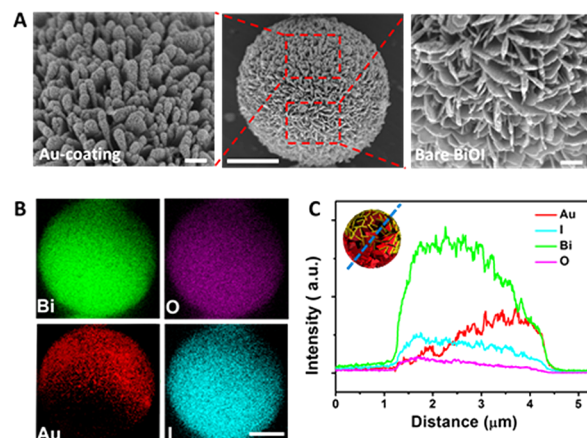


Figure 2. (A) SEM image of BiOI-Au Janus micromotors (center). Scale bar, 1 μm . Left and right images are magnified SEM images of Au-coated and uncoated side of a BiOI particle, respectively. Scale bar, 0.1 μm . (B) EDX images of BiOI-Au Janus micromotors for Bi, O, Au, and I, respectively. Scale bar, 0.5 μm . (C) The intensity distributions of elements Bi, Au, I, and O over the cross section of BiOI-Au Janus micromotors obtained by EDX.

“Off” visible light activation of motors has been demonstrated in Figure 3A,B and Video S2. The micromotors can move at a

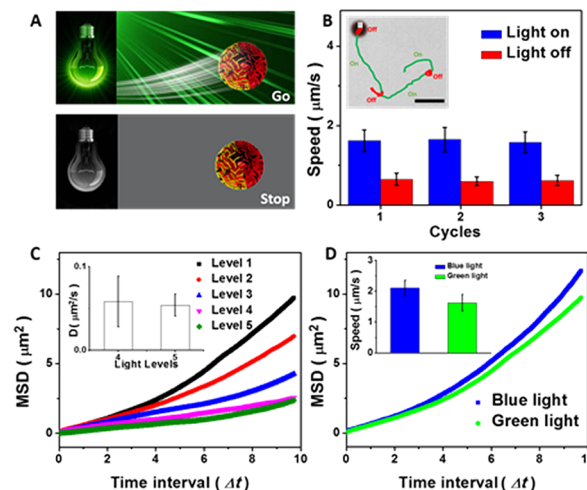


Figure 3. (A) Schematic of BiOI-Au Janus micromotor moving status in pure water with and without green light, respectively. (B) Velocity plot illustrating visible-light-induced 3 cyclic on/off motion of micromotors in water. The inset is the trackline of a BiOI-Au motor (taken from Video S2). Scale bar, 5 μm . (C) Average MSD of micromotors under different green light intensities vs time interval (Δt) analyzed from tracking trajectories (insets are diffusion coefficient values for particles under level 4 and 5 green light). (D) Average MSD of micromotors under green and blue light (insets are the corresponding velocity values).

speed of 1.62 $\mu\text{m/s}$ under level 1 (43 900 lux) green light, but they only exhibit Brownian motion when the light is off, and speeds drop to 0.6 $\mu\text{m/s}$. Such BiOI-based Janus motors have highly repeatable “go/stop” motion controlled by visible light. In addition, it is important to demonstrate the motion of these micromotors under green light with different power levels. The motion of the micromotors changes from Brownian motion to directional motion (parabolic mean-square displacement (MSD)) with increasing luminous flux (Figure 3C). Increasing

the flux of photons of a certain wavelength of light will lead to an enhanced charge separation in BiOI. As a result, more protons are generated and accumulated near the BiOI surfaces to form enhanced gradients which result in high fluid shear velocity around BiOI microsphere, generating directional motion. It is clear from Figure 3C that the BiOI-Au motors exhibit an enhanced directional movement upon exposure to visible light output above level 3 (5410 lux). Note, although level 4 light (2450 lux) has over 24 times higher luminous flux than level 5 light (100 lux), the motors have a similar low diffusion coefficient (Figure 3C inset). The diffusion coefficients here were determined by the equation $D = \text{MSD}/i\Delta t$, where Δt is the time interval. The results illustrate that when the power of green light decreases below level 4, the light intensity has little effect on the propulsion of motors due to the weak photocatalytic activity. The effects of different wavelength visible light (blue, 450–490 nm; green, 510–560 nm) are also investigated. Figure 3D shows that the directional motion of the motors is stronger under blue light than under green light due to the stronger blue light absorption of BiOI.²³

To confirm the propulsion mechanism of motors, the self-propelled motion of the BiOI-based Janus micromotors with different metal layers was systematically investigated by velocity and MSD analysis. Figure 4A,B shows that different coatings

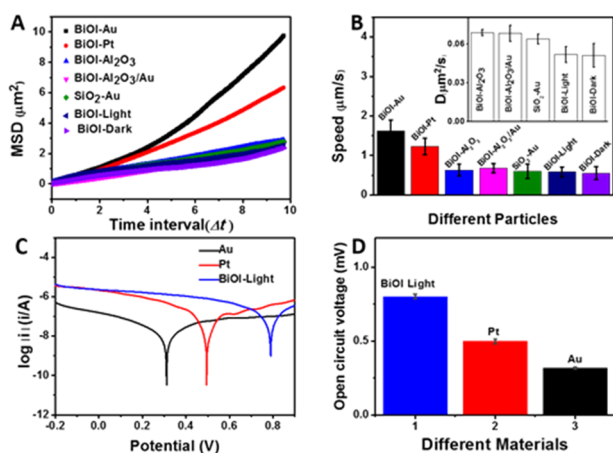


Figure 4. (A) MSD and (B) velocities of different particles in different conditions. Light condition, 43 900 lux green light. (B inset) The corresponding diffusion coefficients of particles with nondirectional motion. (C) Tafel plots and (D) open-circuit voltage of Au, Pt, and BiOI with green illumination (level 1).

have a direct influence on the movement behavior of micromotors. It is found that only BiOI-Au and BiOI-Pt Janus micromotors exhibit directional motion, while other control particles only show Brownian motion, as evidenced by their parabolic or linear MSD curves. Compared to the other particle types that can only move locally, restricted by Brownian motion, the BiOI-noble metal motors have high absolute movement speeds, allowing net motion of the motors. The mixed potentials and open-circuit voltages of BiOI with illumination and different metal electrodes (e.g., Au, Pt) are examined to further explain these results.²⁴ It is clear from Figure 4C that the potential difference of BiOI-Au (478 mV) is much larger than that of BiOI-Pt (294 mV), a similar trend was also observed from the open-circuit voltages (Figure 4D). These findings are consistent with our observation (the MSD and speed of BiOI-Au are much higher than that of BiOI-Pt),

confirming that the directional movement speed of such visible-light-driven Janus micromotor strongly depends on the coated layer due to the self-electrophoresis mechanism.

As we know, Janus particle is commonly propelled by electrophoresis,²⁵ diffusionphoresis,^{6b} thermalphoresis,²⁶ and bubbles.²⁷ A series of control experiments were conducted using plain BiOI microspheres, BiOI- Al_2O_3 , BiOI- $\text{Al}_2\text{O}_3/\text{Au}$, and SiO_2 -Au Janus particles to further validate the propulsion mechanism. Note, in our system, there are no bubbles even under very high intensity. Figure 4B shows that the plain BiOI microsphere does not exhibit obvious directional motion both with and without light. The possible reason is the large size (2–4 μm diameter) and the weak photocatalytic activity of BiOI without metal coating. It is noted that the thermal heating of the solution also exhibits negligible effects on the Brownian motion of bare BiOI particles. Moreover, porous SiO_2 -Au Janus particles (2.0 μm diameter) were used as a control to investigate the effects of asymmetric thermal gradients induced by local heating of the Au coating under visible light. The diffusion coefficient of SiO_2 -Au Janus microspheres is close to that of the plain BiOI particles but no obvious directional motion is observed. This indicates that noble metal coated microspheres under such visible light illumination do not undergo thermophoretic motion (Figure 4B and inset). Finally, the effects of an insulating layer on BiOI-based micromotors were studied. Figure 4B indicates that the BiOI- Al_2O_3 microspheres display a similar diffusion coefficient to plain BiOI. Analogously, BiOI- $\text{Al}_2\text{O}_3/\text{Au}$ microspheres cannot move by the self-electrophoretic mechanism due to the insulating barrier to electrons between the BiOI and Au coating. This also indicates that the photocatalytic activity of BiOI side is not strong enough to propel the motors. Accordingly, the mechanism is not diffusionphoresis. The above results clearly demonstrate the self-electrophoretic mechanism of propulsion for BiOI-metal Janus micromotors. In addition, the motors can still move in 1 mM NaCl solution with a decreased speed of 1.16 $\mu\text{m/s}$ and stop moving in 1 mol/L NaCl solution, which also confirms the self-electrophoretic mechanism. Particularly, the BiOI-Au motor display enhanced propulsion in the presence of biomolecules such as glucose. The speeds of motors go up to 2.6 $\mu\text{m/s}$ in 10 mM glucose solution, promising a great potential in future diverse practical applications. In addition, such motors also show an interesting aggregation behavior under visible light, as shown in Figure S2.

In conclusion, we demonstrate environmentally friendly visible-light-driven BiOI-based Janus micromotors. The self-propelled Janus micromotors are powered by photocatalytic reactions using two of the most common energy sources from nature: visible light and water. The propulsion of such micromotors is based on the self-electrophoresis mechanism and can be adjusted by wavelength and power of visible light. Further efforts will be focused on realizing the use of sunlight to propel motors and promoting the propulsion.

■ ASSOCIATED CONTENT

📄 Supporting Information

The Supporting Information is available free of charge on the ACS Publications website at DOI: 10.1021/jacs.6b09863.

Experimental details; Figures S1 and S2 (PDF)

Video S1, BiOI-Au Janus micromotor with and without green light exposure in pure water (AVI)

Video S2, on/off visible light activation of BiOI-Au Janus micromotor (AVI)

AUTHOR INFORMATION

Corresponding Authors

*mcblyren@scut.edu.cn

*caiyip@scnu.edu.cn

ORCID

Biye Ren: 0000-0003-0131-8750

Yuepeng Cai: 0000-0003-4028-9358

Notes

The authors declare no competing financial interest.

ACKNOWLEDGMENTS

The project receives financial support from the NSFC (21674039, 21471061, and 21671071), China Postdoctoral Science Foundation (2016M602481), NSFC of Guangdong Province (2014A030311001), and Guangdong Provincial Department of Science and Technology (2015B010135009).

REFERENCES

- (1) (a) Gao, W.; Wang, J. *ACS Nano* **2014**, *8*, 3170–3180. (b) Sánchez, S.; Soler, L.; Katuri, J. *Angew. Chem., Int. Ed.* **2015**, *54*, 1414–1444. (c) Guix, M.; Mayorga-Martinez, C. C.; Merkoçi, A. *Chem. Rev.* **2014**, *114*, 6285–6322. (d) Wu, Z.; Lin, X.; Si, T.; He, Q. *Small* **2016**, *12*, 3080–3093. (e) Moo, J. G. S.; Pumera, M. *Chem. - Eur. J.* **2015**, *21*, 58–72. (f) Li, J.; Rozen, I.; Wang, J. *ACS Nano* **2016**, *10*, 5619–5634. (g) Wang, W.; Duan, W.; Ahmed, S.; Mallouk, T. E.; Sen, A. *Nano Today* **2013**, *8*, 531–554. (h) Abdelmohsen, L. K. E. A.; Peng, F.; Tu, Y.; Wilson, D. A. *J. Mater. Chem. B* **2014**, *2*, 2395–2408.
- (2) (a) Paxton, W. F.; Kistler, K. C.; Olmeda, C. C.; Sen, A.; St. Angelo, S. K.; Cao, Y.; Mallouk, T. E.; Lammert, P. E.; Crespi, V. H. *J. Am. Chem. Soc.* **2004**, *126*, 13424–13431. (b) Wong, F.; Sen, A. *ACS Nano* **2016**, *10*, 7172–7179.
- (3) (a) Vilela, D.; Parmar, J.; Zeng, Y.; Zhao, Y.; Sánchez, S. *Nano Lett.* **2016**, *16*, 2860–2866. (b) Singh, V. V.; Kaufmann, K.; de Ávila, B. E.-F.; Karshalev, E.; Wang, J. *Adv. Funct. Mater.* **2016**, *26*, 6270–6278.
- (4) (a) Ma, X.; Jang, S.; Popescu, M. N.; Uspal, W. E.; Miguel-López, A.; Hahn, K.; Kim, D.-P.; Sánchez, S. *ACS Nano* **2016**, *10*, 8751–8759. (b) Gao, W.; Pei, A.; Dong, R.; Wang, J. *J. Am. Chem. Soc.* **2014**, *136*, 2276–2279.
- (5) (a) Peng, F.; Tu, Y.; van Hest, J. C. M.; Wilson, D. A. *Angew. Chem.* **2015**, *127*, 11828–11831. (b) Wilson, D. A.; Nolte, R. J. M.; van Hest, J. C. M. *Nat. Chem.* **2012**, *4*, 268–274.
- (6) (a) Abdelmohsen, L. K. E. A.; Nijemeisland, M.; Pawar, G. M.; Janssen, G.-J. A.; Nolte, R. J. M.; van Hest, J. C. M.; Wilson, D. A. *ACS Nano* **2016**, *10*, 2652–2660. (b) Ma, X.; Jannasch, A.; Albrecht, U.-R.; Hahn, K.; Miguel-López, A.; Schäffer, E.; Sánchez, S. *Nano Lett.* **2015**, *15*, 7043–7050. (c) Sengupta, S.; Dey, K. K.; Muddana, H. S.; Tabouillot, T.; Ibele, M. E.; Butler, P. J.; Sen, A. *J. Am. Chem. Soc.* **2013**, *135*, 1406–1414. (d) Ma, X.; Hortelão, A. C.; Patiño, T.; Sánchez, S. *ACS Nano* **2016**, *10*, 9111–9122.
- (7) (a) Li, T.; Li, J.; Zhang, H.; Chang, X.; Song, W.; Hu, Y.; Shao, G.; Sandraz, E.; Zhang, G.; Li, L.; Wang, J. *Small* **2016**, *12*, 6098. (b) Peyser, K. E.; Tottori, S.; Qiu, F.; Zhang, L.; Nelson, B. J. *Chem. - Eur. J.* **2013**, *19*, 28–38.
- (8) (a) Calvo-Marzal, P.; Sattayasamitsathit, S.; Balasubramanian, S.; Windmiller, J. R.; Dao, C.; Wang, J. *Chem. Commun.* **2010**, *46*, 1623–1624. (b) Loget, G.; Kuhn, A. *J. Am. Chem. Soc.* **2010**, *132*, 15918–15919.
- (9) (a) Ahmed, D.; Baasch, T.; Jang, B.; Pane, S.; Dual, J.; Nelson, B. *J. Nano Lett.* **2016**, *16*, 4968–4974. (b) Ahmed, S.; Wang, W.; Bai, L.; Gentekos, D. T.; Hoyos, M.; Mallouk, T. E. *ACS Nano* **2016**, *10*, 4763–4769. (c) Wang, W.; Castro, L. A.; Hoyos, M.; Mallouk, T. E. *ACS Nano* **2012**, *6*, 6122–6132.
- (10) (a) Ibele, M.; Mallouk, T. E.; Sen, A. *Angew. Chem., Int. Ed.* **2009**, *48*, 3308–3312. (b) Xuan, M.; Wu, Z.; Shao, J.; Dai, L.; Si, T.; He, Q. *J. Am. Chem. Soc.* **2016**, *138*, 6492–6497.
- (11) Mou, F.; Li, Y.; Chen, C.; Li, W.; Yin, Y.; Ma, H.; Guan, J. *Small* **2015**, *11*, 2564–2570.
- (12) Wu, Z. G.; Si, T. Y.; Gao, W.; Lin, X. K.; Wang, J.; He, Q. *Small* **2016**, *12*, 577–582.
- (13) Palagi, S.; Mark, A. G.; Reigh, S. Y.; Melde, K.; Qiu, T.; Zeng, H.; Parmeggiani, C.; Martella, D.; Sanchez-Castillo, A.; Kapernaum, N.; Giesselmann, F.; Wiersma, D. S.; Lauga, E.; Fischer, P. *Nat. Mater.* **2016**, *15*, 647–653.
- (14) Ichihashi, M.; Ueda, M.; Budiyo, A.; Bito, T.; Oka, M.; Fukunaga, M.; Tsuru, K.; Horikawa, T. *Toxicology* **2003**, *189*, 21–39.
- (15) König, K.; Tadir, Y.; Patrizio, P.; Berns, M. W.; Tromberg, B. J. *Hum. Reprod.* **1996**, *11*, 2162–2164.
- (16) Zou, Z.; Ye, J.; Sayama, K.; Arakawa, H. *Nature* **2001**, *414*, 625–627.
- (17) Cheng, H.; Huang, B.; Dai, Y. *Nanoscale* **2014**, *6*, 2009–2026.
- (18) Pan, M.; Zhang, H.; Gao, G.; Liu, L.; Chen, W. *Environ. Sci. Technol.* **2015**, *49*, 6240–6248.
- (19) Zhu, L.; He, C.; Huang, Y.; Chen, Z.; Xia, D.; Su, M.; Xiong, Y.; Li, S.; Shu, D. *Sep. Purif. Technol.* **2012**, *91*, 59–66.
- (20) Wang, K.; Jia, F.; Zhang, L. *Mater. Lett.* **2013**, *92*, 354–357.
- (21) (a) Yu, C.; Cao, F.; Li, G.; Wei, R.; Yu, J. C.; Jin, R.; Fan, Q.; Wang, C. *Sep. Purif. Technol.* **2013**, *120*, 110–122. (b) López-Tenllado, F. J.; Hidalgo-Carrillo, J.; Montes, V.; Marinas, A.; Urbano, F. J.; Marinas, J. M.; Ilieva, L.; Tabakova, T.; Reid, F. *Catal. Today* **2017**, *280*, 58–64.
- (22) (a) Yu, C.; Yu, J. C.; Fan, C.; Wen, H.; Hu, S. *Mater. Sci. Eng., B* **2010**, *166*, 213–219. (b) Ye, L.; Su, Y.; Jin, X.; Xie, H.; Zhang, C. *Environ. Sci.: Nano* **2014**, *1*, 90–112. (c) Lee, W. W.; Lu, C.-S.; Chuang, C.-W.; Chen, Y.-J.; Fu, J.-Y.; Siao, C.-W.; Chen, C.-C. *RSC Adv.* **2015**, *5*, 23450–23463.
- (23) Xiao, X.; Zhang, W.-D. *J. Mater. Chem.* **2010**, *20*, 5866–5870.
- (24) Wang, Y.; Hernandez, R. M.; Bartlett, D. J.; Bingham, J. M.; Kline, T. R.; Sen, A.; Mallouk, T. E. *Langmuir* **2006**, *22*, 10451–10456.
- (25) Mou, F. Z.; Kong, L.; Chen, C. R.; Chen, Z. H.; Xu, L. L.; Guan, J. G. *Nanoscale* **2016**, *8*, 4976–4983.
- (26) Xuan, M.; Wu, Z.; Shao, J.; Dai, L.; Si, T.; He, Q. *J. Am. Chem. Soc.* **2016**, *138*, 6492–6497.
- (27) Li, Y.; Mou, F.; Chen, C.; You, M.; Yin, Y.; Xu, L.; Guan, J. *RSC Adv.* **2016**, *6*, 10697–10703.